Study on the Physical and Chemical Characteristics and Sources of Atmospheric Single Particles in Weifang During the 2022 Winter Olympic Games and the Winter Paralympic Games

Zhe Chang[1], Jian Gao[2], Wenjun Li[2], Jinying Li[2], and Lili Song[1(✉)]

[1] School of Ecological Technology and Engineering, Shanghai Institute of Technology, Shanghai 201418, China
songLL713@163.com

[2] Atmospheric Environment Institute, Chinese Research Academy of Environmental Sciences, Beijing 100012, China

Abstract. In order to evaluate the effectiveness of air quality assurance measures during the 2022 Beijing Winter Olympic Games and the Winter Paralympic Games, samples of atmospheric particulates in Weifang City during the 2022 Winter Olympic Games and the Winter Paralympic Games were collected to analyze the level of air pollution during the Winter Olympic Games and the Winter Paralympic Games. The computer-controlled scanning electron microscopy and energy spectrum system (CCSEM-EDX) was used to analyze the morphology characteristics of particulates, the type and quantity proportion of particulates, and the quantity-particle size distribution of particulates. The results show that the air quality during the 2022 Winter Olympic Games and the Winter Paralympic Games is better than that in the same historical period of 2020 and 2021, the control measures are effective.

Keywords: Atmospheric particulates · Source analysis · Winter Olympic Games and Winter Paralympic Games · Computer-controlled scanning electron microscope

1 Introduction

The 24th Winter Olympic Games and the 13th Winter Paralympic Games were held in Beijing, China, from February 4 to 20 and March 4 to 13, 2022. To ensure the air quality during the period, the Weifang Municipal Bureau of Ecological Environment has taken measures to promote clean energy for heating in winter, shut down coal-fired power plants and other coal-fired facilities, prohibit the setting off of fireworks and firecrackers, and prohibit foreign vehicles and other trucks with a load of more than 4 tons from driving into the urban area of Beijing to ensure the air quality. According to the announcement released on the official website of the Ministry of Ecology and

N. Akhtar et al. (Eds.): PMIS 2023, AHIS 8, pp. 884–897, 2023.
https://doi.org/10.2991/978-94-6463-200-2_92

Environment of China, the average concentration of $PM_{2.5}$ in Beijing-Tianjin-Hebei and surrounding areas is 52 $\mu g/m^3$ decreased by 20%, and the number of heavily polluted days decreased by more than 90%.

The traditional source analysis method uses the method of combining chemistry and mathematical statistics, taking the conservation of mass as the basic assumption, and represents the characteristic value (concentration, composition, etc.) of the atmospheric particulate pollutant sample collected by the receptor by the corresponding characteristic value of the pollutant source emission in the receptor area using linear superposition to identify the source of atmospheric particulate matter, thus effectively control air pollution and improve air quality. However, classical source analysis has problems such as collinearity, the uncertainty of source spectrum, and uncertainty of the actual state of particulate matter in the atmosphere, and it is difficult to establish the local source characteristic spectrum. Sample analysis is not accurate at low environmental concentrations of pollutants. Single-particle analysis can provide the morphology, mixing state, aging degree, and element composition of single particles suspended in the ambient air, and can more intuitively observe the sample, thus intuitively identifying the source of particles. The sample required for single particle analysis is small, so it can be studied at low pollutant concentrations. The trend of improving air quality in China has attracted much attention. Using the single particle analysis method to study the aging process, optical properties, hygroscopicity, heterogeneous and heterogeneous reactions, and single particle mixing state of different types of particles is of great significance for revealing the transformation of atmospheric particles and evaluating the climate effect of atmospheric particles [1–4]. The traditional electron microscope analysis needs a manual operation, which can only analyze about 1000 particles per hour, and the analysis efficiency is low; The computer-controlled scanning electron microscope and energy spectrum system (CCSEM-EDX) can obtain energy spectrum and image information of thousands of particles per hour, significantly improving the efficiency of particle analysis. Currently, scholars have used CCSEM-EDX to study the change of the mass concentration of specific types of particulate matter with time in a small area, the spatial variability of the mass and composition of regional particulate matter, and the seasonal change of particulate matter [5–8].

Weifang City is located in the western region of the Shandong Peninsula. It is located at the core of the peninsula's urban agglomeration. It is an industrial mountain city. The energy consumption is enormous. The energy structure is still dominated by fossil fuel combustion and extensive industrial processing. In this study, Weifang City was selected as the research site, and the UNC passive sampler was used to collect single particle samples. The sampling period was from January 28 to March 28, 2022, and the sampling frequency was 5–7 days. The IntelliSEM EPAS intelligent electronic microscope system is used to characterize the physical and chemical properties of particulate matter samples, compare the change characteristics of particle quantity, particle size distribution, and type in different periods, and then analyze the change characteristics of particle source in different time periods of the 2022 Weifang Winter Olympic Games and the Winter Paralympic Games, and evaluate the effectiveness of air quality assurance measures for the Winter Olympic Games.

Fig. 1. Sample collection location and surrounding conditions.

2 Materials and Methods

2.1 Sampling Sites and Sample Collection

Weifang City is adjacent to Qingdao City and Yantai City in the east, Zibo City and Dongying City in the west, Linyi City and Rizhao City in the south, Bohai Sea in the north, 183 km from the provincial capital Jinan in the west and 410 km from the capital Beijing in the northwest (Fig. 1). The sampling point is located on the top of the old Weifang Environmental Protection Bureau building. The UNC passive sampler is placed on the annular floor and fixed on the building with L-shaped support. The passive sampler does not need power, b but mainly relies on gravity sedimentation, diffusion, and inertia to collect particulate matter in the ambient air [9]. The collection time of each sample is determined by the start and end time of the Winter Olympic Games and the Winter Paralympic Games and the air quality during the sampling period. The collection frequency is 5–7 days. During the period from January 28 to March 28, 2022, a total of 10 samples were collected (Table 1), which can be divided into five stages: before the Winter Olympic Games (Sample 1), during the Winter Olympic Games (Sample 2–4), after the Winter Olympic Games and before the Winter Paralympic Games (Sample 5–6), during the Winter Paralympic Games (Sample 7–8) and after the Winter Paralympic Games (Sample 9–10).

2.2 Sample Analysis

Through the IntelliSEM EPAS system of RJ Lee Group, the equivalent diameter of 10 groups of samples is 0.2 ~ 50 μm. To better compare the pollution degree of different samples during collection, each sample has analyzed 24.4mm2 in the center of the sample, classified the particles according to the element composition, and statistically analyzed the quantity and particle size of each type of particle in the two samples, determined the analysis carbon (C), oxygen (O), sodium (Na), magnesium (Mg), aluminum (Al), silicon (Si), phosphorus (P), sulfur (S), chlorine (Cl), potassium (K), calcium (Ca), titanium (Ti), vanadium (V) The relative abundance of 31 elements: chromium (Cr), manganese

Table 1. Table captions should be placed above the tables.

Sample number	Sampling time
Sample 1	5:00, January 28 to 4:30, February 3
Sample 2	5:00, February 3 to 4:30, February 9
Sample 3	5:00, February 9 to 4:30, February 15
Sample 4	5:00, February 15 to 4:30, February 21
Sample 5	5:00, February 21 to 4:30, February 26
Sample 6	5:00, February 26 to 4:30, March 3
Sample 7	5:00, March 3 to 4:30, March 8
Sample 8	5:00, March 8 to 4:30, March 14
Sample 9	5:00, March 14 to 4:30, March 21
Sample 10	5:00, March 21 to 4:30, March 28

(Mn), iron (Fe), cobalt (Co), nickel (Ni), copper (Cu), zinc (Zn), arsenic (As), bromine (Br), tin (Sn), antimony (Sb), barium (Ba), gold (Au), cerium (Ce), praseodymium (Pr), neodymium (Nd), europium (Eu), gadolinium (Gd).

2.2.1 Data Handling

In this study, ten samples were analyzed, and the morphometric energy spectrum information of 67103 particles was obtained. Although CCSEM technology has greatly improved the efficiency of sample testing, it is found that the recognition efficiency of carbon particles and other types is not high in the process of processing. There are errors such as repeated recognition of identical particles, false recognition due to the damage of polycarbonate bottom film, and false edge tracing of particles due to contrast problems. In this paper, the particles obtained from the CCSEM test are manually checked, including deleting the particles identified incorrectly and repeatedly and redrawing the particles incorrectly traced.

According to the synchronous observation data of the air monitoring station of Weifang Ecological Environment Center and the air quality historical data of the air quality release software, the air quality from January 28 to March 28, 2020–2022, is analyzed. Then the air quality during the sampling period and the same historical period is evaluated.

2.2.2 Classification Method of Particulate Matter

According to the classification method of Okada et al. [10] based on the results of SEM-EDX analysis, the formula P (X) = X/(sum of relative abundance of elements except for carbon and oxygen) × 100%. Particles with a P (X) value greater than 65% are called rich "X" particles. Particles with a P (X) value less than 65% are classified as "the element with the highest P value + the element with the second highest P value".

Table 2. Average mass concentration of $PM_{2.5}$ and PM_{10} in the same period of the history of Cangzhou Winter Olympic Games and Winter Paralympic Games.

Month	Type	2020	2021	2022
February 4 to February 20	$PM_{2.5}$	52.7 μg/m^3	44.9 μg/m^3	45.7 μg/m^3
	PM_{10}	68.6 μg/m^3	75.8 μg/m^3	63.9 μg/m^3
March 4 to March 13	$PM_{2.5}$	55.8 μg/m^3	72.2 μg/m^3	50.5 μg/m^3
	PM_{10}	91.4 μg/m^3	119.3 μg/m^3	118.2 μg/m^3

This paper applies this method and combines the morphology of particles to classify particles.

3 Results and Analysis

3.1 Air Pollution During the Winter Olympic Games and the Winter Paralympic Games

The average mass concentrations of $PM_{2.5}$ and PM_{10} during the same period of the Winter Olympic Games and the Winter Paralympic Games in Weifang City are shown in Table 2. Except for the slightly higher concentration of PM_{10} during the Winter Paralympic Games due to dust weather, other air quality is significantly better than that during the same period of history. The air quality control measures in Weifang City during the 2022 Beijing Winter Olympic Games and the Winter Paralympic Games are effective.

The air quality of Weifang from January 28 to March 28, 2020–2022, is shown in Fig. 2. During the 2022 Beijing Winter Olympic Games, the number of days of air pollution in Weifang City was two days, which was significantly lower than the 4 days in the same period of Weifang City in 2020, slightly higher than the one day in the same period of Weifang City in 2021. The degree of pollution was lower than in the same period in 2020, which was the same as that in 2021, which proved that the air quality control measures during the Winter Olympic Games were effective. The number of pollution days during the 2022 Winter Paralympic Games was two days, significantly lower than the four days in the same period in 2020 and 2021. The results showed that the air quality control measures during the Winter Paralympic Games were effective.

3.2 Physical and Chemical Characteristics of Atmospheric Particulates

3.2.1 Micro Topography Feature Analysis

The scanning electron microscope image of particulate matter is shown in Fig. 3. The C-peak of carbon-rich particles is very high, mainly from coal combustion, motor vehicles, and cooking emissions. Pollen grains mainly contain C elements, and some contain a small amount of P and S elements. Soot particles are an aggregate of multiple carbonaceous particles, generally considered to come from fossil fuel combustion and biomass combustion emissions [11]. Organic particles are regular spherical particles containing C

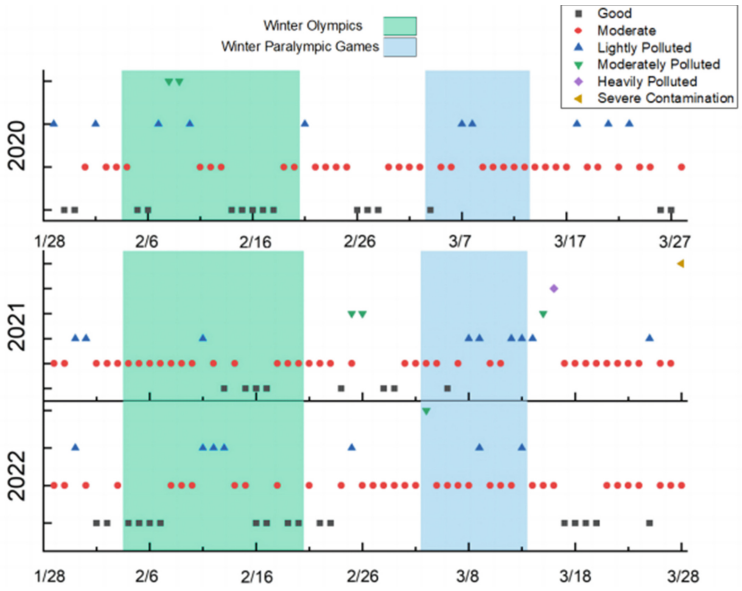

Fig. 2. Air quality change chart of Weifang from January 28 to March 28, 2020–2022.

elements, mainly from fossil fuel and biomass combustion [12]. Mineral particles mainly come from construction dust, road dust and crust dust, most of which come from dust storms or long-distance transportation of dust [13]. The fiber is composed of organic fiber and inorganic fiber. The organic fiber is composed of microplastics and natural organic fiber particles. The inorganic fiber is mainly artificial mineral fiber, asbestos, calcium sulfate, and metal fiber particles [14]. Several types of fibers are found in all samples, including artificial mineral fiber, metal fiber, sulfate fiber, microplastics, and calcium sulfate fiber. Sea salt particles mainly come from the sea or evaporation lakes, and the main elements are Na, Cl, and S, which usually have cubic NaCl crystal form, and also have aged amorphous particles. It is generally believed that in some humid coastal environments, cubic sea salt crystals tend to form amorphous sea salt particles after aging [15]. This paper finds fresh sea salt particles and aged sea salt particles. The potassium-rich particles in the atmosphere mainly come from the outdoor combustion and cooking emissions of agricultural biomass, mainly composed of K, N, Cl, and S, and are usually irregular in shape [16]. The metal particles come from heavy industry, fuel combustion, vehicle, and rail wear [17]. The metal particles from the combustion source are often spherical, while the metal particles from the wear source are often polygonal. Weifang has found a variety of metal particles containing Fe, Zn, Cr, As, Sn, Sb, Ni, Ti, and Ba elements and droplets of particles. Most of the spherical iron particles are combustion processes of steelmaking containing chromium. The metal particles of iron may come from the emissions of diesel engines, chromium oxide may exist in the filler of brake linings and can also be burned from lubricating oil [18], tin-rich particles may come from the fuel combustion of port vessels [19], titanium balls may come from the pigment manufacturing process [20], and irregular titanium sheets may come from road

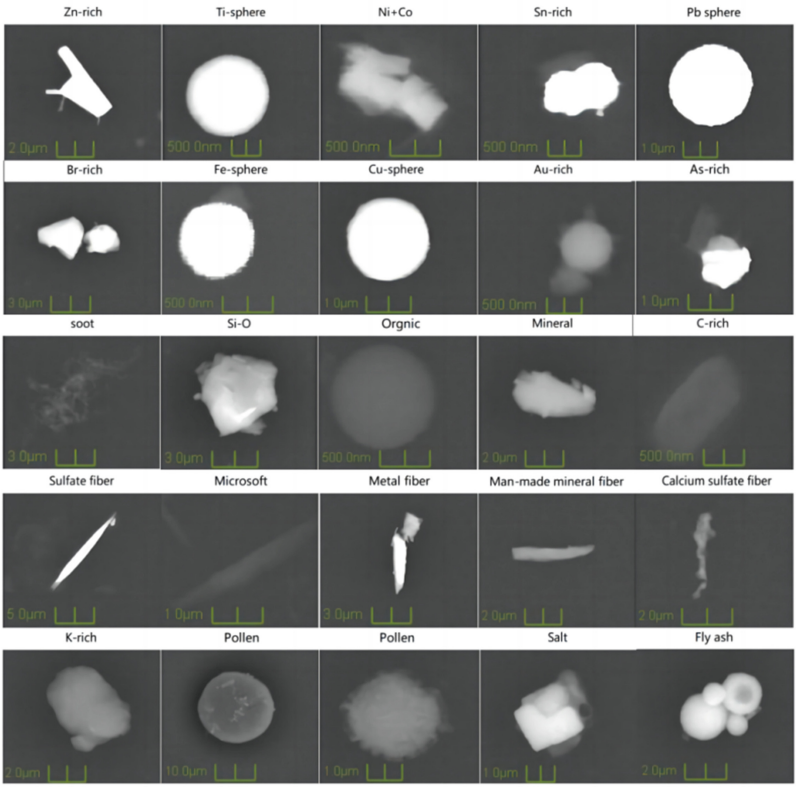

Fig. 3. SEM image of particulate matter.

dust and wear of tires and brakes [21]. Sulfur-rich particles are irregular in shape and volatile under the electron beams, usually forming a "foam-like" structure. Coal-fired fly ash particles are spherical particles containing Si and Al and a small amount of Ca, Ti, Mn and Fe. These particles are usually produced by coal combustion for cooking, heating, industrial activities, and power plants [22].

3.2.2 Micro Topography Feature Analysis

The daily average quantity concentration of particulate matter and the variation characteristics of the quantity-particle size distribution of particulate matter are shown in Fig. 4 and Fig. 5. The daily average amount of particulate matter during the Winter Olympic Games is significantly lower than that before and after the Winter Olympic Games. The air quality is mainly affected by fine particulate matter. The effect of air quality control measures during the Winter Olympic Games is obvious; During the Paralympic Games, affected by the dust weather on March 4 and March 14, the average amount of particulate matter per day increased significantly, and the air quality was mainly affected by coarse particulate matter. On the whole, the air quality during the Winter Olympic Games was better than that during the Winter Paralympic Games.

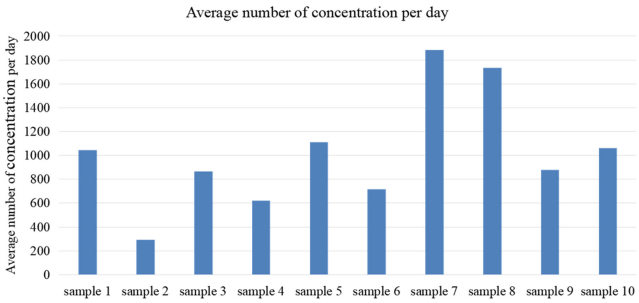

Fig. 4. Daily average particle quantity concentration

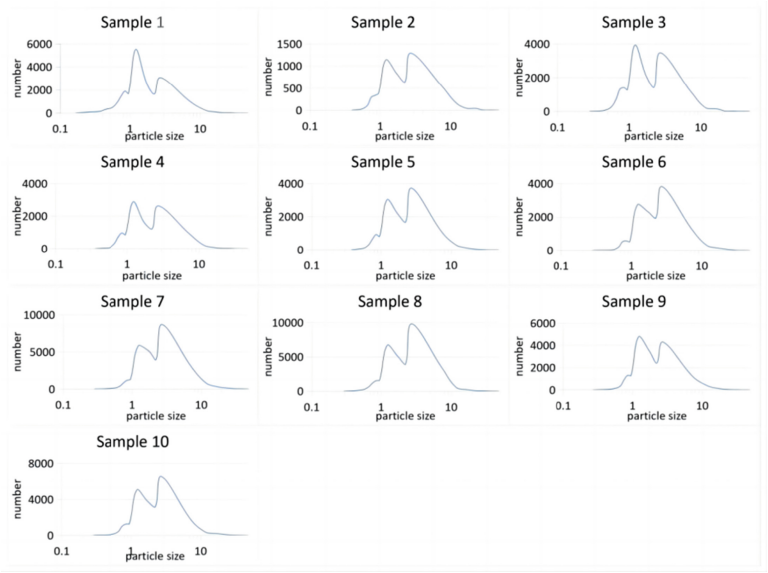

Fig. 5. Quantity - particle size distribution diagram

3.3 Research on the Traceability of Atmospheric Particulate Matter

The variation characteristics of particulate matter types during the study are shown in Fig. 6. The main types of particulate matter in Weifang are Al-rich, Ca-rich, Si-rich, C-rich, salt, sulfate, and Fe-rich particulate matter. There are more types of metal particles, indicating that there are more industrial types in Weifang. Mineral particles accounted for more than 60% of the coarse particles in the samples from Weifang City. During and after the Winter Paralympic Games (samples 7–10), Al-rich, Si-rich, and Ca-rich particles increased significantly, indicating that they were affected by the dust weather. The variation characteristics of particulate matter types during the study are shown in Fig. 6. The main types of particulate matter in Weifang are Al-rich, Ca-rich, Si-rich, C-rich, salt, sulfate, Fe-rich, K-rich, fly ash particles. There are more types of metal

particles, indicating that there are more industrial types in Weifang. Mineral particles accounted for more than 60% of the coarse particles in the samples from Weifang City.

During the Winter Paralympic Games, the Weifang Municipal People's Government carried out special rectification of construction debris and dust, used high-pressure cleaning vehicles or wet sweeping vehicles to clean the primary and secondary roads, banned the burning of straw, dead leaves, fireworks, and firecrackers, and carried out inspections on the burning of bulk coal, construction sites, catering and barbecue enterprises, and critical sections of the road in the no-fire zone, and continuously strengthened the control of key pollution sources. The proportion of carbon particles before the Winter Olympic Games was 40.93%, much higher than that of the samples during the Winter Olympic Games and the Winter Paralympic Games. The proportion of metal particles and coal fly ash in the samples from February 9 to 15 was lower than that of the samples from February 21 to 26. The proportion of metal particles and carbon particles in the samples from March 8 to 14 was lower than that of the samples from March 21 to 28. The results showed that the control measures for motor vehicles, coal emissions and industry during the Winter Olympic Games and the Winter Paralympic Games were effective.

The daily mean values of the proportion and quantity of iron and titanium spheres in the total particulate matter of Weifang are shown in Fig. 7. Most iron balls come from the combustion process of steelmaking [18], while titanium balls come from pigment manufacturing [20]. The proportion of iron balls in the samples during the Winter

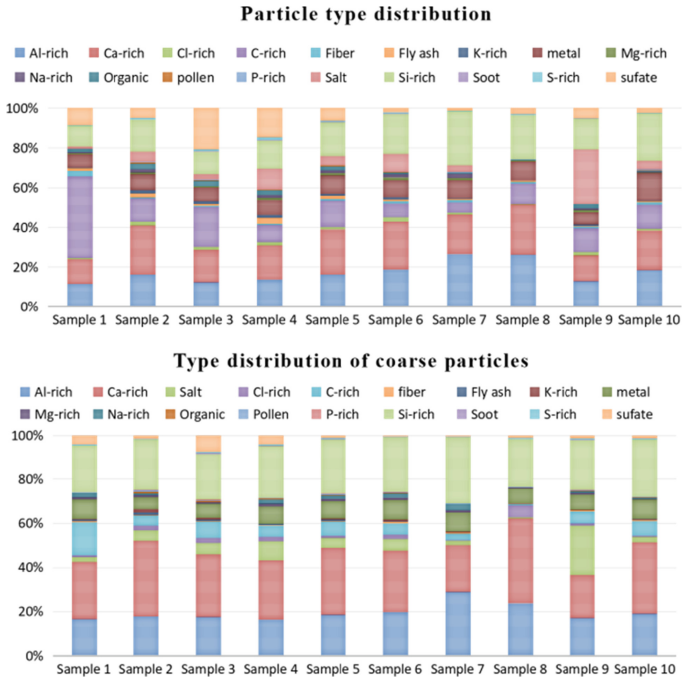

Fig. 6. Distribution of particulate matter type.

Olympic Games is higher than that after the Winter Paralympic Games, and the average amount of particulate matter per day is lower than that after the Winter Paralympic Games, which indicates that the control effect of steel making industry is better during the Winter Olympic Games, but the control effect of other pollution sources is better, resulting in a higher proportion; The proportion of titanium balls in the samples of the Winter Olympic Games is higher than that before and after the Winter Olympic Games, but the average amount of particulate matter per day is lower than that before and after the Winter Olympic Games. The results show that the control effect of the pigment manufacturing industry is better during the Winter Olympic Games. Still, the control effect of other pollution sources is better, resulting in a higher proportion. The proportion of iron balls in the samples during the Winter Paralympic Games is lower than that after the Winter Paralympic Games, but the average number of iron balls per day is higher than that after the Winter Paralympic Games, which means that the dust weather affects its proportion, but the control effect of steel making industry during the Winter Paralympic Games is not obvious; The proportion of titanium balls in the samples during the Winter Paralympic Games and the daily average particle quantity is lower than those in other stages. The overall control effect of the pigment manufacturing industry during the Winter Paralympic Games is good.

The variation characteristics of element abundance and the variation characteristics of element abundance ratio during the study period are shown in Fig. 8 and Fig. 9. The identifying element of soil dust is Si, and that of construction cement dust is Ca [23]. The abundance of Si/Ca and Si decreased slightly during the Winter Olympic Games, and the abundance of Ca increased significantly. During the Winter Olympic Games, the soil dust's impact decreased, and the impact of construction cement dust increased; The abundance of Si and Ca increased significantly during and after the Winter Paralympic Games, and the content of Si/Ca increased significantly during and

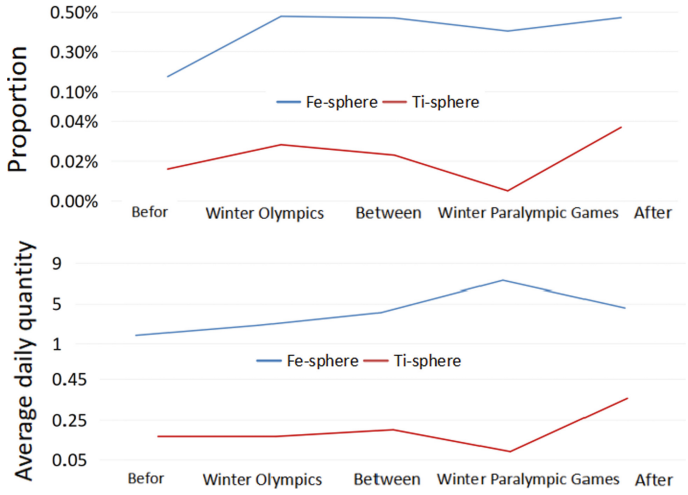

Fig. 7. Daily average of quantity and proportion of iron spheres and titanium spheres in total particulate matter

after the Winter Paralympic Games. During and after the Winter Paralympic Games, the content of Si/Ca was affected by soil dust. The abundance of V/Cu and V elements is usually used to determine the contribution of shipping emissions [24, 25]. The mass fraction of V elements in diesel and gasoline vehicles is 0.01% and 0%, respectively [26], and 2.7–30.7% in particulate matter emitted by shipping [27]. Suppose the V element is considered a shipping emission because the abundance of V/Cu and V element increases during the Winter Paralympic Games. It is considered that the effect of shipping emission control during the Winter Paralympic Games is not noticeable.

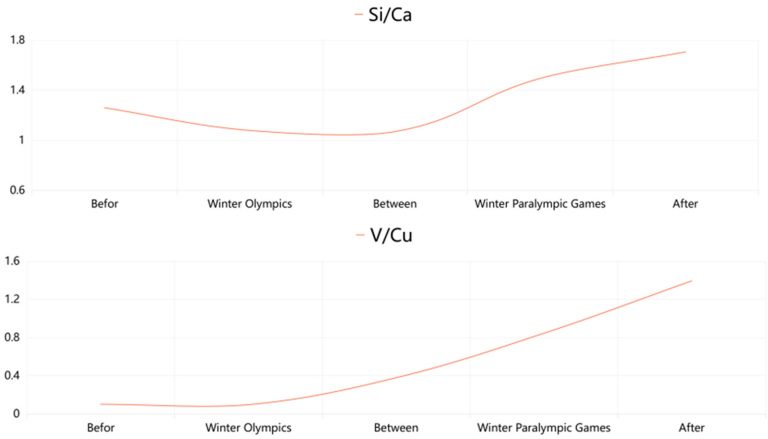

Fig. 8. Comparative diagram of element abundance.

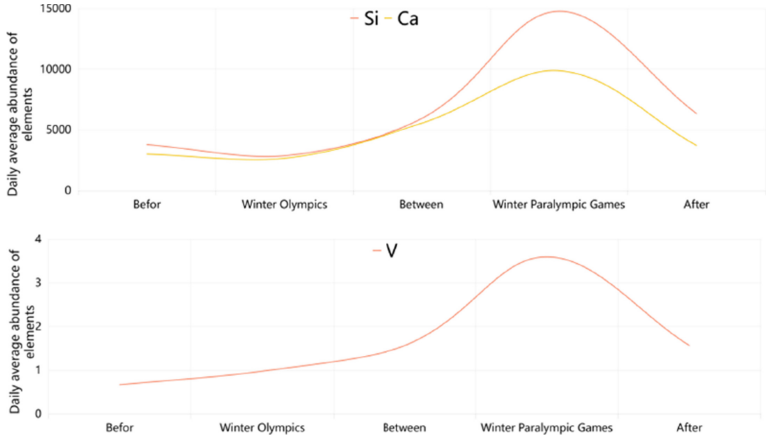

Fig. 9. Element abundance.

4 Conclusion

The average mass concentration, pollution days, and pollution degree of $PM_{2.5}$ and PM_{10} during the 2022 Beijing Winter Olympics and Winter Paralympic Games in Weifang City are generally lower than the historical period of 2020 and 2021, indicating that the air quality of Weifang City during the Winter Olympics and Winter Paralympic Games is better than the historical period of 2020 and 2021. The air quality control measures are effective, and the pollution process during the Winter Olympics is mainly affected by fine particles; The pollution process during the Winter Olympic Games is mainly affected by coarse particles.

The air quality during the Winter Olympic Games is mainly affected by fine particles. The daily average amount of particulate matter is significantly lower than before and after the Winter Olympic Games. The effect of air quality control measures during the Winter Olympic Games is obvious; Affected by dust weather during the Paralympic Games, the air quality is mainly affected by coarse particles, and the average daily amount of particles is significantly increased. The air quality during the Winter Olympic Games is better than that during the Winter Paralympic Games.

There are many kinds of metal particles in Weifang, indicating many industrial types in Weifang. The carbon particulate matter in the samples before the Winter Olympic Games is much higher than that in the samples after the Winter Paralympic Games, indicating that the control measures from motor vehicles and coal emissions during the Winter Olympic Games and the Winter Paralympic Games are effective. In the samples of the Winter Olympic Games and the Winter Paralympic Games, the proportion of non-metallic particles, coal-fired fly ash and carbonaceous particles in the samples is significantly lower than that before and after the Winter Olympic Games and the Winter Paralympic Games, and the control measures for motor vehicles, coal emissions and industry during the Winter Olympic Games and the Winter Paralympic Games have apparent effects. Through the research on the change of the proportion of titanium and iron balls in total particulate matter and the average daily quantity, the research found that the control effect of the steel-making industry and pigment manufacturing during the Winter Olympic Games was better, while the control effect of the steel making industry during the Winter Paralympic Games was not obvious, and the overall control effect of the pigment manufacturing industry was better. Through the study of the values of Si/Ca and V/Cu and the element abundance of Si, Ca, and V, it is found that the control effect of shipping emissions during the Winter Paralympic Games is not obvious; During the Winter Olympic Games, the impact of construction cement dust is enhanced, and the impact of soil dust is weakened. During the Winter Paralympic Games and after the Winter Paralympic Games, the impact of soil dust is enhanced.

References

1. Du H , Li J , Chen X , et al. Modeling of aerosol property evolution during winter haze episodes over a megacity cluster in northern China: roles of regional transport and heterogeneous reactions of SO2[J]. *Atmospheric Chemistry and Physics*, 2019, 19(14):9351-9370.

2. Liu L, Zhang J, Zhang Y, et al. Persistent residential burning-related primary organic particles during wintertime hazes in North China: insights into their aging and optical changes [J]. *Atmospheric Chemistry and Physics*, 2021, 21(3):2251-2265.
3. Mengyuan Zhang, Longyi Shao, Tim Jones, Xiaolei Feng, Shuoyi Ge,Cheng-Xue Yang, Yaxin Cao, Kelly BéruBé, Daizhou Zhang,Atmospheric iron particles in PM2.5 from a subway station, Beijing, China[J],*Atmospheric Environment*, 2022, 283:119175-.
4. Ault A P , Peters T M , Sawvel E J , et al. Single-particle SEM-EDX analysis of iron-containing coarse particulate matter in an urban environment: sources and distribution of iron within Cleveland, Ohio.[J]. *Environmental Science & Technology*, 2012, 46(8):4331–4339.
5. Wang M, Hu T, Wu F, et al. Characterization of PM 2.5 carbonaceous particles with a high-efficiency SEM: A case study at a suburban area of Xi'an[J]. *Aerosol Science and Engineering*, 2021, 5: 70–80.
6. Sawvel E J, Willis R ,West R R , et al. Passive sampling to capture the spatial variability of coarse particles by composition in Cleveland, OH[J]. *Atmospheric Environment*, 2015, 105(mar.):61–69.
7. Kumar P , Hopke P K ,Raja S , et al. Characterization and heterogeneity of coarse particles across an urban area[J]. *Atmospheric Environment*, 2012, 46(none):449–459.
8. Byeon S H, Willis R, Peters T M. Chemical characterization of outdoor and subway fine (PM2. 5–1.0) and coarse (PM10–2.5) particulate matter in Seoul (Korea) by Computer-Controlled Scanning Electron Microscopy (CCSEM)[J]. *International Journal of Environmental Research and Public Health*, 2015, 12(2): 2090–2104.
9. MD Castillo, Wagner J, Casuccio G S , et al. Field testing a low-cost passive aerosol sampler for long-term measurement of ambient PM2.5 concentrations and particle composition [J]. *Atmospheric Environment*, 2019, 216:116905-.
10. Li W J, Shao L Y, Shi Z B, et al. Physical and chemical characteristics of individual mineral particles in an urban fog episode[J]. *Huan Jing ke Xue= Huanjing Kexue,* 2008, 29(1): 253–258.
11. Xing J, Shao L , Rong Z , et al. Individual particles emitted from gasoline engines: Impact of engine types, engine loads and fuel components[J]. *Journal of Cleaner Production*, 2017, 149:461-471.
12. Xing J, Shao L, Zhang W, et al. Morphology and composition of particles emitted from a port fuel injection gasoline vehicle under real-world driving test cycles[J]. *Journal of Environmental Sciences*, 2019, 76: 339-348.
13. OR Hernández, Boit K D , Blanco E , et al. Hazardous thoracic and ultrafine particles from road dust in a Caribbean industrial city[J]. *Urban Climate*, 2020, 33(100655):1–11.
14. Li Y, Shao L , Wang W , et al. Airborne fiber particles: Types, size and concentration observed in Beijing[J]. *The Science of the Total Environment*, 2020, 705(Feb.25):135967.1–135967.9.
15. Li W , Shao L . Characterization of mineral particles in winter fog of Beijing analyzed by TEM and SEM[J]. *Environmental Monitoring and Assessment*, 2010, 161(1-4):565-573.
16. Giordano M , Espinoza C , Asa-Awuku A . Experimentally measured morphology of biomass burning aerosol and its impacts on CCN ability[J]. *Atmospheric Chemistry and Physics*, 15, 4(2015–02–20), 2015, 14(9):12555–12589.
17. Moreno T, Martins V, Querol X, et al. A new look at inhalable metalliferous airborne particles on rail subway platforms[J]. *Science of the Total Environment*, 2015, 505: 367-375.
18. Charron A , Polo-Rehn L , Besombes J L , et al. Identification and quantification of particulate tracers of exhaust and non-exhaust vehicle emissions[J]. *Atmospheric Chemistry and Physics*, 2019, 19(7):5187-5207.
19. Morillas H , Marcaida I , Maguregui M , et al. Identification of metals and metalloids as hazardous elements in PM2.5 and PM10 collected in a coastal environment affected by diffuse contamination[J]. *Journal of Cleaner Production*, 2019, 226(JUL.20):369–378.

20. Huang Y , Cheng X . Characteristics and sources of atmospheric particulate matter and health risk in Southwest China[J]. *Asian Atmospheric Pollution*, 2022: 409–433.
21. Apeagyei E, Bank M S , Spengler J D . Distribution of heavy metals in road dust along an urban-rural gradient in Massachusetts[J]. *Atmospheric Environment*, 2011, 45(13):2310-2323.
22. Wang W, Shao L, Li J, et al. Characteristics of individual particles emitted from an experimental burning chamber with coal from the lung cancer area of Xuanwei, China[J]. *Aerosol and Air Quality Research*, 2019, 19(2): 355-363.
23. Chow J C, Watson J G, Kuhns H, et al. Source profiles for industrial, mobile, and area sources in the Big Bend Regional Aerosol Visibility and Observational study[J]. *Chemosphere*, 2004, 54(2): 185-208.
24. Pey J, Pérez N, Cortés J, et al. Chemical fingerprint and impact of shipping emissions over a western Mediterranean metropolis: Primary and aged contributions[J]. *Science of the total environment*, 2013, 463: 497-507.
25. Tolis E I, Saraga D E, Filiou K F, et al. One-year intensive characterization on PM2. 5 nearby port area of Thessaloniki, Greece[J]. *Environmental Science and Pollution Research*, 2015, 22: 6812–6826.
26. Huang H, Zhang J, Hu H, et al. On-road emissions of fine particles and associated chemical components from motor vehicles in Wuhan, China[J]. *Environmental Research*, 2022, 210: 112900.
27. Moldanová J, Fridell E, Popovicheva O, et al. Characterisation of particulate matter and gaseous emissions from a large ship diesel engine[J]. *Atmospheric Environment*, 2009, 43(16): 2632-2641.